LA-UR-93-2640 Revised 9/27/93

Title: **H^- and D^- Scaling Laws for Penning Surface-Plasma Sources**

Author(s): H. Vernon Smith, Jr., Paul Allison, and Joseph D. Sherman

Submitted to: Accepted for publication in the Review of Scientific Instruments Volume 65 (tentatively scheduled for the January, 1994 issue)

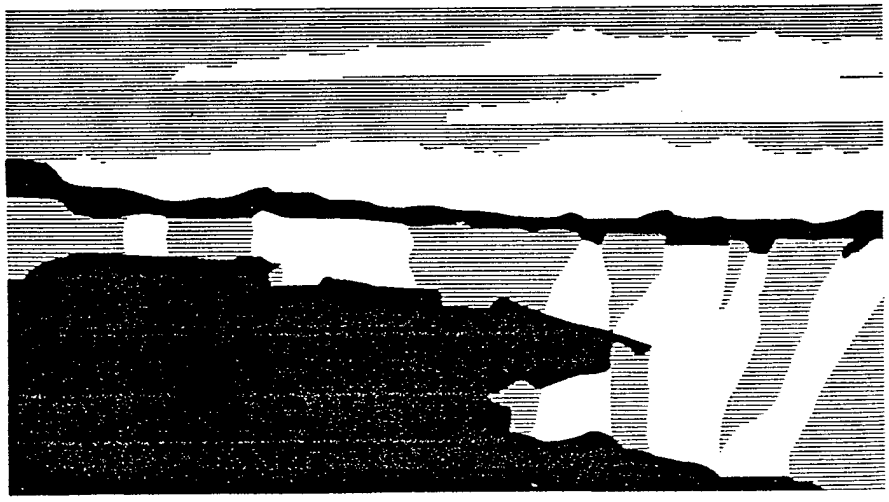

Los Alamos
NATIONAL LABORATORY

Accession Number: 4884

Publication Date: Sep 27, 1993

Title: H- and D- Scaling Laws for Penning Surface-Plasma Sources

Personal Author: Smith, H.V.; Allison, P.; Sherman, J.D.

Corporate Author Or Publisher: Los Alamos National Laboratory, Los Alamos, NM 87545 Report Number: LA-UR-93-2640

Comments on Document: Accepted for publication in the Review of Scientific Instruments Volume 65 (tentatively scheduled for the January, 1994 issue)

Descriptors, Keywords: H- D- Scale Law Penning Surface Plasma Ion

Pages: 00028

Cataloged Date: Feb 10, 1994

Document Type: HC

Number of Copies In Library: 000001

Record ID: 28622

H^- AND D^- SCALING LAWS FOR PENNING SURFACE-PLASMA SOURCES *

H. Vernon Smith, Jr., Paul Allison, and Joseph D. Sherman

Los Alamos National Laboratory, Los Alamos, NM 87545

ABSTRACT

The small-angle source (SAS), 4X source, and 8X source are Penning surface-plasma sources (SPS) that produce high-current, high-brightness H^- ion beams for accelerator applications. The scaling from the SAS (1X source) to the 4X source, and from the 4X source to the 8X source is at least as good as predicted by the scaling laws. In many instances, the scaling is better than predicted, particularly in the critical area of the efficiency with which H^- ions are produced per unit of discharge power. Using $\zeta = j_{H^-}/F_C$, where F_C is the cathode power load, $\zeta_{4X} \approx 2\ \zeta_{SAS}$ and $\zeta_{8X} \approx 1.5\ \zeta_{4X}$. The j_{H^-} scaling is at least as good as predicted by the scaling laws – we have been able to produce the predicted H^- current in both the 4X and the 8X sources. The SAS was scaled up in size to the 4X source, and the 4X source was scaled up in size to the 8X source, on the assumption that the effective $kT_{H^-} = 5$ eV. These temperature scalings appear to be obeyed. We also assumed that $kT_{H^-} = kT_{D^-}$ and $j_{D^-} = j_{H^-}/\sqrt{2}$. The temperature scaling appears to be obeyed, and the D^- current scaling appears to be even better than assumed, namely $j_{D^-} \approx j_{H^-}$.

INTRODUCTION

Experimental development of Penning SPS[1] at Los Alamos[2-8] has proceeded towards high duty-factor (df) H^- beams.[6,8] An early version[2] of the SAS[3] operates dc for many hours at an H^- emission current density $j_{H^-} = 80$ mA/cm^2 (emitter area A = 0.05 cm^2; $I_{H^-} = 4$ mA). This result shows that dc operation at reasonable current density is possible; in fact, this dc operation is considerably more power efficient than that for pulsed, high-current density (3000 mA/cm^2). Although the 4X source[4,5] can operate at a discharge df of 6%,[6] the beam quality degrades at higher df for unknown reasons. The addition of N_2 gas to the 4X source discharge overcomes this problem at 2% beam df. Another serious problem is handling the power from the co-extracted electron beam. A tungsten extraction electrode operates with minimum damage for 2% H^- beam df, and a scheme which allows the electrons to pass through the extraction electrode to an auxiliary e^- beam dump appears feasible. The electron-handling scheme will be helped by the reduction in the e^-/H^- ratio accomplished using a conical-collar arrangement.[9]

While developing the 4X source to deliver a 2% df H^- beam, we noticed that the H^- beam-emission scaling from the SAS to the 4X source is more favorable than the scaling laws predict. This led us to the conclusion that a cooled 8X ion source may produce 50- to 100-mA dc H^- beams from a 4-mm-diam aperture. Thus, we designed and built a low-duty-cycle 8X source prototype for physics testing.

BACKGROUND

The Penning SPS, as first reported by Dudnikov,[1] was widely recognized for its potential to produce bright H^- beams for accelerator applications. Since that time, several groups have contributed to its development, including those at Novosibirsk,[10] Brookhaven,[11] Rutherford Lab,[12] and Los Alamos.[2-8] With slit emitters, emission-current densities of 3-4 A/cm^2 (Ref. 10)

and H^- temperatures of 1 eV (Refs. 13, 14) can be achieved. The extracted emission-current density degrades with circular emitters, but they produce the brightest Penning SPS H^- beams.[7]

The H^- production mechanisms have been reviewed by Belchenko.[15] Two are proposed, both involving surface production of H^- followed by collisions with atoms. In the first, H^- ions are produced on the cesium-coated cathode and injected into the discharge. Resonant-charge-exchange collisions with low-temperature $H°$ in the discharge produce the low-temperature H^- extracted from the source. The second mechanism, a supplement to the first, is the production of H^- by $H°$ bombardment of the cesium-coated, near-emitter anode walls. Subsequent collisions of these H^- with $H°$ near the emitter increases the H^- current produced by this method.

The duty factor of the 1X source is limited by the power density on the electrodes ($\approx$10 kW/cm^2 on the cathode to produce 100 mA of H^-). In addition, the transport system between the source and the accelerator must be carefully designed to avoid large emittance growth.[16] We have constructed and tested a series of Penning SPS with increasingly large discharge dimensions in our attempts to overcome these problems. This paper reports our experience with these sources on the test stand. We note that the operational reliability and reproducibility of the 4X source is considerably improved over the SAS (our 1X source).

PENNING SPS SCALING LAWS

For the Penning SPS scaling laws, we adopt the scaling laws for high-density plasmas.[17] The high-density scaling laws state that if the source size is increased by the factor K_1 and the gas density, magnetic field, and cathode current density are decreased by the factor $1/K_1$, then the discharge voltage and particle temperatures will be the same, but the particle densities ($H°$, H^+, e^-, H^-, etc.) will be reduced by the factor $1/K_1$. Also, the particle- and current-density ratios (e.g., j_{H^-}/j_{e^-}) remain unchanged. The H_2 particle density, magnetic field, and cathode current density are

set to the required values by adjusting the H_2 gas flow, arc-magnet current, and discharge current, respectively.

PREDICTED AND OBSERVED SCALING FROM THE SAS TO THE 4X SOURCE

The SAS produces 150 mA of H^- with 0.006×0.017 π cm mrad (rms normalized) emittance from a 0.8×7.0 mm^2 slit emitter;[7] from a 0.25-cm-diam circular emitter, it produces 82 mA of H^- with an rms emittance of 0.0053×0.0056 π cm mrad.[7] These performance levels are achieved at 0.5% discharge df (1-ms-long pulses at 5 Hz). The SAS cathode's instantaneous power load is 10-20 kW/cm^2, far too high to consider dc operation. To lower the instantaneous cathode power loading, and to accommodate a 5.4-mm-diam emitter (the SAS cathode-cathode gap is 4.3 mm), we built the 4X source.[4-7] It is also a Penning SPS, but with larger discharge chamber dimensions. To give perspective for the source size increases discussed in this paper, Fig. 1 shows a photograph of the SAS, 4X, and 8X source cathodes.

The Penning SPS geometry is shown in Fig. 2. The dimensions for the SAS and the 4X source are shown in Table I. The SAS measured and 4X source predicted performances are, with the exception of j_{H^-}, F_C, and ζ, from Table I of Ref. 4. The 4X source measured performance is from Ref. 7. A schematic drawing of the SAS is given in Fig. 5 of Ref. 3; a schematic of the 4X source is in Fig. 1 of Ref. 5. To produce a given amount of H^- current (I_{H^-}) with the 4X source, its discharge current must be adjusted by the factor $K_2 = 0.87$ where

$$I_{H^-} = 160 \text{ mA} = (\pi R^2 K_2 \ / \ K_1)\, j_{H^-} \qquad (1)$$

with 2R the 4X source emitter diameter (5.4-mm diam), $j_{H^-} = 3.2$ A/cm^2 (the SAS emission-current density), and $K_1 = 4$. The linear K_2 scaling is an experimental observation. The design and measured 4X source performances are compared in Table I. The drift region in the SAS is 1-mm thick; in the 4X source it is 4-mm thick. The scaling predictions are generally accurate. We increased the discharge depth (W in Fig. 2) from 12 to 17 mm to achieve a quiescent H^- beam,[7] and we decreased the extraction gap from 4.7 to 3.6 mm to meet the I_{H^-} goal. These results are

quite encouraging, especially the cathode power density load, F_C, which is lower than our design value. It is useful to define a cathode power efficiency $\zeta = j_{H^-}/F_C$. In units of $(mA/cm^2)/(kW/cm^2)$, $\zeta_{SAS} = 160$, but $\zeta_{4X} = 290$, nearly twice as high (Table I). This improvement in ζ is not expected from the scaling laws, but it is very important.

The H^- beam emittance scaling is also of vital importance. When we designed the 4X source, we assumed that the effective H^- temperature kT_{H^-} would remain the same as for the SAS slit emitter results, namely $kT_{H^-} = 5$ eV. If ε is the rms normalized emittance and m is the ion mass, using

$$\varepsilon = (R/2)\sqrt{kT_{H^-}/mc^2} \qquad (2)$$

we anticipate $\varepsilon = 0.01\ \pi$ cm mrad . Our measured result is $0.019 \times 0.020\ \pi$ cm mrad for a 150-mA, 23-keV H^- beam implying a kT_{H^-} closer to 20 eV. However, if the emitter radius is halved, ε drops to $0.0049\ \pi$ cm mrad for a 50-mA, 29-keV H^- beam giving $kT_{H^-} = 5.3$ eV. This implies that ε varies more like R^2 than R, a result also observed for the H^- beam measured from a cusp-field volume source.[18] We note that the effective kT_{H^-} is the same in the SAS and the 4X source, ≈5 eV. We measured the H° temperature in the SAS and 4X sources.[19] For the scaled discharge currents, 180 A for both the SAS and 4X sources, the measured kT_{H^0} values are ≈1.8 eV (Figs. 3 and 4 of Ref. 19). Thus, the temperature scaling holds for those species that we have measured.

We note that for the 4X source the true H^- temperature at emission is ≈1 eV (Ref. 13), considerably lower than the ≈5 eV effective kT_{H^-} determined from the emittance measurements. Apparently, the H^- temperature is "spoiled" somewhere along the transport from the emission aperture to the emittance scanner 12 cm away by an effect such as perveance fluctuations in the extraction gap, space-charge-induced emittance growth, or extractor aberrations. Thus, for the emittance scaling we use the effective kT_{H^-} value of 5 eV, not the H^- temperature in the plasma, 1 eV.

We also measured[19] the plasma density in the SAS and 4X sources. The result at the scaled currents is 1.7 x 10^{14} cm^{-3} for the SAS and 1.6 x 10^{14} cm^{-3} for the 4X source. This is, of course, a violation of the scaling laws – the plasma density in the 4X source should be lower than that in the SAS by a factor of ≈4. The origin of this discrepancy is unknown. We note that the greater-than-predicted plasma density in the 4X source does not translate into an improved emission current density, since $j_{H^-} \approx 700$ mA/cm^2 for the 4X source and $j_{H^-} \approx 3200$ mA/cm^2 for the SAS.

The 4X source produces 250 mA of pulsed H^- beam with rms normalized emittance 0.015 × 0.029 π cm mrad from a slit emitter[6] and 63 mA of H^- with 0.0061 × 0.0060 π cm mrad emittance from a 0.26-cm-diam circular emitter. This circular emitter result is for a discharge df of 2.3% and a H^- beam df of 2.0%. In other experiments, where an H^- beam was not extracted, the discharge df was as high as 6%.[6] The instantaneous cathode power loading for these 4X source runs was ~2.5 kW/cm^2, still high but considerably reduced from the 10-20 kW/cm^2 for the SAS.

PREDICTED SCALING FROM THE 4X SOURCE TO THE 8X SOURCE

Although the 4X source allows the use of large circular emitters, 50- to 100-mA dc H^- beams are unlikely because the cathode power load is ≈ 2.5 kW/cm^2. We built the 8X source to see if there is further beneficial scaling of the cathode power efficiency, ζ, so that the cathode power loading can be reduced to ≈1 kW/cm^2 and still produce the desired H^- current. The 4X source results[7] in Table II are used for the 8X source design. Using the (arbitrary) requirement that I_{H^-} = 130 mA and

$$I_{H^-} = 130 \text{ mA} = (\pi R^2 K_2 / K_1)\, j_{H^-} \qquad (3)$$

where 2R is the 8X source emitter diameter (5.4-mm-diam from our emittance scaling discussed below), j_{H^-} = 940 mA/cm^2, and K_1 = 2 gives K_2 = 1.2. The original 8X source design for assumed 480-A discharge current and 570-mA/cm^2 j_{H^-} is given in column 2 of Table II. Scaling down the emitter radius R to 1.3 mm should produce 30 mA of H^- current (column 4 of Table II). For both 8X source designs, we assume that the effective kT_{H^-} remains the same as for the 4X

source 0.26-cm-diam emitter results, 5 eV. From eq. 2 we calculate $\varepsilon = 0.010\ \pi$ cm mrad for the 8X source with R = 0.27 cm. For R = 0.13 cm we calculate $\varepsilon = 0.005\ \pi$ cm mrad.

OBSERVED SCALING FROM THE 4X SOURCE TO THE 8X SOURCE

An uncooled, pulsed 8X source (Fig. 3) was built and tested so that we could compare its measured performance with its predicted performance (Table II). The 8X source plasma chamber is a cube with 3.4-cm sides. The H^- ions traverse a 0.8-cm-thick drift region before being extracted through a circular emitter and formed into a beam. The H^- beam current and emittance, and the power efficiency ζ, are of particular interest. The 4X source and 8X source performances are measured using the same test stand. An electric-sweep emittance scanner[20] is used for the emittance measurements, and a Faraday cup is used for the current measurements.

First, we tested the 8X source with a 0.26-cm-diam emitter. The 8X source pulsed measurements are for 1.1-ms-long arc pulses at a repetition rate of 5 Hz. The best overall H^- current and emittance (i.e., H^- beam brightness) is illustrated in Fig. 4. Figure 4a shows the current oscillogram for a 25-keV, 37-mA-H^- beam from the 8X source; Fig. 4b shows the x-plane phase-space plot (the y-plane phase-space plot is nearly identical) for that same beam. The z axis is along the beam direction. The contour levels in Figs. 4b and 5b are 1%, 5%, 10%, 20%, 30%, 40%, and 50% of the maximum phase-space density. The rms emittance is $0.0056 \times 0.0055\ \pi$ cm mrad. Column 5 of Table II gives the consistent set of source parameters for this beam [the 88-V, 490-A discharge produces the 37 mA, $0.0056 \times 0.0055\ \pi$ cm mrad H^- beam]. To reduce the H^- beam noise N_2 gas is added to the 8X source discharge. The best values of I_{H^-}, j_{H^-}, ε, effective kT_{H^-}, and ζ are given in footnotes b, d, and f of Table II. The emittance values given in Table II are for the extraction voltage which gives the lowest emittance – if the extraction voltage is set at the design value, the resulting emittance is higher than that given in Table II.

The 8X source H^- performance with a 0.54-cm-diam emitter was also measured. The H^- current oscillogram for a 120-mA beam from the 8X source is shown in Fig. 5a. The x-plane

phase-space plot for this beam is given in Fig. 5b (the y-plane phase-space plot is nearly identical); the consistent set of source parameters for the beam in Fig. 5 is given in column 3 of Table II. The best values of I_{H^-}, j_{H^-}, ε, effective kT_{H^-}, and ζ for the 0.54-cm-diam emitter are given in footnotes a, c, and e of Table II.

The design and measured 8X source performances are compared in columns 2 and 3 of Table II for the 0.54-cm-diam emitter and in columns 4 and 5 for the 0.26-cm-diam emitter. The 8X source meets all of the scaling law predictions for the smaller emitter and nearly all of them for the larger emitter. The principal exception is the cathode power efficiency ζ, which is larger than our design value. In units of mA/kW, the measured $\zeta_{8X} = 640$ is nearly 50% higher than the design value (Table II). Thus, the scaling laws underpredict the 8X source ζ value scaled from the 4X source results, just as they underpredicted the 4X source ζ value scaled from the SAS results. We also note that for both the 0.54- and 0.26-cm-diam emitters the 8X source H_2 gas flow is $\approx$50 % lower than predicted by the scaling laws.

The H^- beam emittance scaling is also of interest. In designing the 8X source, the effective H^- temperature kT_{H^-} is assumed to be the same as that of the 4X source, 5 eV. From eq. (2), we anticipate $\varepsilon = 0.01\ \pi$ cm mrad. For a 110-mA-, 35-keV-H^- beam, we measure $0.011 \times 0.012\ \pi$ cm mrad, giving $kT_{H^-} = 6.2$ eV. If the emitter radius is halved, ε drops to $0.0048\ \pi$ cm mrad for a 31-mA-, 25-keV-H^- beam, giving $kT_{H^-} = 5.1$ eV. Thus, the effective kT_{H^-} does appear to scale correctly from the 4X to the 8X source. We have measured the H^- temperature at emission by the slit-diagnostic technique.[13,21] The result for discharge currents near the scaled values, 180 A for the 4X source and 480 A for the 8X source, is $kT_{H^-} \approx 1$ eV for both sources. Thus, the H^- temperature in the 4X and 8X source plasmas is identical.

Belchenko et al. report[22] dc operation of an H^- planotron at $F_C = 1$ kW/cm^2. Thus, $j_{H^-} \geq 640$ mA/cm^2 might be possible for dc operation of a Penning source. The 4X source time-average j_{H^-} is now only 24 mA/cm^2 (with a minimally-cooled cathode). The cooled, dc 8X source[8] (called the CW 8X Source) is based on the pulsed-8X-source test results reported here.

PREDICTED AND OBSERVED D^- SCALING

The assumed scaling for D^- is $j_{H^-} = \sqrt{2}\, j_{D^-}$ and $kT_{D^-} = kT_{H^-}$. We measured the 8X source D^- performance with the 0.26-cm-diam emitter. The procedure is to first start the source up on H_2 and optimize the H^- emittance by adjusting the cesium flow and magnetic field, then switch to D_2. The residual gas in the HCTS pump box is monitored with a quadrupole mass analyzer before and after the switch to D_2 to ensure that no detectable H_2 gas remains in the hydrogen feed line. We adjust the 8X source parameters to the same discharge current, $\sqrt{2}$ higher magnetic field, and $\sqrt{2}$ lower D_2 flow than H_2 flow (to give the same pressure in the source). We increase the extraction voltage from 25 kV for the H^- measurements to 30 kV for the D^- measurements to make the D^- and H^- beam perveances the same.

The 8X source parameters for the H_2 and D_2 measurements made on the same day are shown in Table III. For D^- operation the minimum magnetic field at which the source discharge will operate is $\sqrt{2}$ times the minimum field needed for H^- operation, confirming that minimal H_2 is present in the D_2 discharge. The H^- and D^- currents are about the same, 33 and 30 mA respectively, for about the same discharge parameters. Thus, the surprising conclusion is that $j_{H^-} \approx j_{D^-}$; that is, the D^- current scaling is more beneficial than assumed.

The x-plane phase-space plots for the H^- and D^- beams in columns 1 and 2 of Table III are shown in Fig. 6 (the y-plane phase-space plots are nearly identical to the x-plane plots). For the 33-mA H^- beam the measured emittance is $0.0055 \times 0.0058\ \pi$ cm mrad. From these H^- measurements we predict that $\varepsilon_{D^-} = 0.0039 \times 0.0041\ \pi$ cm mrad, very close to the measured D^- values of $0.0037 \times 0.0042\ \pi$ cm mrad. Thus, we conclude that the effective $kT_{H^-} \approx$ the effective kT_{D^-}.

It is desirable to achieve high-duty-factor (df) operation, ultimately dc, with a Penning SPS. Two developments may make this goal possible. First, as we have shown in this paper, the H^- beam-emission scaling from the SAS (the 1X device) to the 4X source, and from the 4X source to

the 8X source, is more favorable than the scaling laws predict. Also, the D^- operation is at least as good as predicted by the scaling laws. Second, fringe-field separation of the e^- and H^- beams may make it possible to handle the power of the coextracted e^- beam, especially since a collar arrangement reduces the e^- loading.[9] We have shown that a conical collar reduces the e^-/H^- ratio from $\approx$5/1 to < 1/1 without reducing the H^- current.[9] Although we have not repeated these measurements for D^-, we expect that the e^-/D^- ratio will be reduced by a factor of 5, from 9/1 to < 2/1, with no reduction in the D^- current. We are now testing a source designed for dc operation.[8,23-24]

REFERENCES

* Work supported and funded by the US Department of Defense, Army Strategic Defense Command under the auspices of the US Department of Energy.

1. V. G. Dudnikov, "Surface-Plasma Source of Negative Ions With Penning Geometry," Transactions of the Fourth All-Union Conference on Charge-Particle Accelerators (Nauk Publishers, Moscow, 1975), Vol. 1, p. 323.

2. P. W. Allison, IEEE Trans. Nucl. Sci. **NS-24**, 1594 (1977).

3. P. Allison and J. D. Sherman, AIP Conf. Proc. **No. 111**, 511 (1984).

4. H. V. Smith, Jr., P. Allison, and J. D. Sherman, AIP Conf. Proc. **No. 111**, 458 (1984).

5. H. V. Smith, Jr., P. Allison, and J. D. Sherman, IEEE Trans. Nucl. Sci. **NS-32**, 1797 (1985).

6. H. V. Smith, Jr., N. M. Schnurr, D. H. Whitaker, and K. E. Kalash, Proc. 1987 Particle Accelerator Conf., IEEE Catalog No. 87CH2387-9, 301 (1987).

7. H. V. Smith, Jr., J. D. Sherman, and P. Allison, Proc. 1988 Linac Conf., CEBAF report no. CEBAF-R-89-001, 164 (1989).

8. H. V. Smith, Jr., et al., "CW 8X Ion Source Development," AIP Conf. Proc. **No. 287**, 1993 (in press).

9. H. V. Smith, Jr., and P. Allison, Rev. Sci. Instrum. **64**, 1394 (1993).

10. V. G. Dudnikov, Rev. Sci. Instrum. **63**, 2660 (1992).

11. K. Prelec, Nucl. Instr. and Meth. **144**, 413 (1977).

12. R. Sidlow and N. D. West, proc. Third European Particle Accelerator Conf., Vol. 2 (Editions Frontieres, Gif-sur-Yvette Cedex, France, 1992) pp 1005-7.

13. J. D. Sherman, H. V. Smith, Jr., C. Geisik, and P. Allison, Rev. Sci. Instrum. **62**, 2314 (1991).

14. V. G. Dudnikov and G. E. Derevyankin, "The Art of High-Brightness Ion Beam Production," AIP Conf. Proc. **No. 287**, 1993 (in press).

15. Yu. I. Belchenko, Rev. Sci. Instrum. **64**, 1385 (1993).

16. R. R. Stevens, Jr., "High-Current Negative-Ion Beam Transport," AIP Conf. Proc. **No. 287**, 1993 (in press).

17. C. E. Muehe, J. Appl. Phys. **45**, 82 (1974).

18. J. W. Kwan, G. D. Ackerman, O. A. Anderson, C. F. Chan, W. S. Cooper, G. J. deVries, K. N. Leung, A.F. Lietzke, and W. F. Steele, Rev. Sci. Instrum. **61**, 369 (1990).

19. H. V. Smith, Jr., P. Allison, and R. Keller, AIP Conf. Proc. **No. 158**, 181 (1987).

20. P. W. Allison, J. D. Sherman, and D. B. Holtkamp, IEEE Trans. Nucl. Sci. **NS-30**, 2204 (1983).

21. H. V. Smith, Jr., J. D. Sherman, C. Geisik, and P. Allison, Rev. Sci. Instrum. **63**, 2723 (1992).

22. Yu. I. Belchenko, G. I. Dimov, V. G. Dudnikov, and A. S. Kupriyanov, Revue Phys. Appl. **23**, 1847 (1988).

23. H. V. Smith, Jr., P. Allison, C. Geisik, D. R. Schmitt, J. D. Schneider, and J. E. Stelzer, "Initial Operation of the CW 8X H^- Ion Source Discharge," Proc. 1993 Particle Accelerator Conf., IEEE Catalog No. 93CH3279-7, 1993 (in press).

24. H. V. Smith, Jr., P. Allison, C. Geisik, D. R. Schmitt, J. D. Schneider, and J. E. Stelzer, "A dc Penning Surface-Plasma Source," Rev. Sci. Instrum., 1993 (in press).

Table I. Comparison of the 4X source predicted and measured H^- performance.

	SAS Measured	4X Source Design	4X Source Actual
Cathode-cathode gap (L), mm	4.3	17	17
Discharge slot depth (W), mm	3	12	17
Discharge slot length (T), mm	12	16	16
Discharge magnetic field, kG	2.2	0.5	0.4
Emitter dimensions, mm	0.5×10	$5.4\ \phi$	$5.4\ \phi$
Extraction gap, mm	2.5	4.7	3.6
Extraction voltage, kV	22	29	29
Discharge voltage, V	100	100	110
Discharge current, A	180	230	180
Maximum H^- current, mA	160	160	170
j_{H^-}, mA/cm^2	3200	700	740
F_C (cathode power load), kW/cm^2	20	4.4	2.5
ζ (cathode power efficiency), mA/kW	160	160	290
Discharge duty factor, %	0.5	~ 5	0.5[a]

[a] This source has been operated with discharge duty factor as high as 6%.

Table II. Design and measured 8X source H^- scaling.

	4X Source Measured	Original 8X Source Design	Original 8X Source Measured	Modified 8X Source Design	Modified 8X Source Measured
Cathode gap (L), mm	17	34	-	34	-
Discharge depth (W), mm	17	34	-	34	-
Discharge length (T), mm	16	34	-	34	-
Discharge field, kG	0.4	0.2	0.29	0.2	0.27
Emitter R, mm	1.3	2.7	2.7	1.3	1.3
Extraction gap, mm	3.0	3.2	3.7	3.2	3.0
Extraction voltage, kV	29	35	30	35	25
Discharge voltage, V	92	92	80	92	88
Discharge current, A	180	480	490	480	490
H^- current, mA	50	130	120[a]	30	37[b]
j_{H^-}, mA/cm^2	940	570	520[a]	570	700[b]
H_2 gas flow, Tℓ/s	0.63	1.4	0.72	0.32	0.14
N_2 gas flow, Tℓ/s	-	0.04	0.015	0.01	0.0040
$\varepsilon_{x,y}$, π cm mrad	0.0049	0.010	0.015	0.005	0.0056
	×		×		×
	0.0050		0.014[c]		0.0055[d]
Effective kT_{H^-}, eV	5.3	5	10[c]	5	6.7[d]
$A_{cathode}$, cm^2	5.1	22	-	22	-
F_C, kW/cm^2	2.2	1.3	1.2	1.3	1.3
A_{anode}, cm^2	10	44	-	44	-
F_A, kW/cm^2	0.54	0.33	0.29	0.33	0.33
ζ (j_{H^-}/F_C), mA/kW	440	440	460[e]	440	540[f]

[a] For R = 0.27 cm the maximum I_{H^-} is 150 mA; the maximum j_{H^-}, 650 mA/cm^2.

[b] For R = 0.13 cm the maximum I_{H^-} is 46 mA; the maximum j_{H^-}, 870 mA/cm^2.

[c] In another measurement, ε = 0.011 π cm mrad, giving Effective kT_{H^-} = 6.2 eV.

[d] In another measurement, ε = 0.0048 π cm mrad, giving Effective kT_{H^-} = 5.1 eV.

[e] For a 150 mA H^- beam with I_d = 500 A and V_d = 75V, ζ = 590 mA/kW.

[f] For a 46 mA H^- beam with I_d = 500 A and V_d = 91 V, ζ = 640 mA/kW.

Table III. 8X source H^- and D^- performance measured on the same day. For the D^- beam the source parameters are adjusted to the same discharge current, $\sqrt{2}$ higher magnetic field, $\sqrt{2}$ lower D_2 flow than H_2 flow (to give the same pressure in the source), and 1.2 higher extraction voltage (to match the D^- beam perveance to the H^- beam perveance).

	8X Source H^-	8X Source D^-
Discharge magnetic field, kG	0.27	0.39
Emitter R, mm	1.3	1.3
Extraction gap, mm	3.0	3.0
Extraction voltage, kV	25	30
Discharge voltage, V	73	69
Discharge current, A	500	510
H^-/D^- current, mA	33	30
j_{H^-,D^-}, mA/cm^2	620	570
H_2 gas flow, T*l*/s	0.19	0.14
N_2 gas flow, T*l*/s	0.0042	0.0055
$\varepsilon_{x,y}$, π cm mrad	0.0055×0.0058	0.0037×0.0042
Effective kT_{H^-,D^-}, eV	6.8	6.0
F_C, kW/cm^2	1.1	1.1
ζ_{H^-,D^-} ($j_{H^-,D^-}/F_C$), mA/kW	570	540
$e^-/H^-,D^-$ ratio	5/1	9/1

FIGURE CAPTIONS

Figure 1. A photograph of the SAS, 4X, and 8X source cathodes. The 4X source cathode-cathode gap, 17 mm, is four times the SAS cathode-cathode gap, 4.3 mm. The 8X source cathode-cathode gap, 34 mm, is eight times the SAS cathode-cathode gap.

Figure 2. A schematic that shows the important geometrical dimensions of the Penning SPS source. L is the cathode-cathode gap, W is the discharge depth (along the beam direction z), and T (out of the paper) is the discharge length. The magnetic field direction is also shown.

Figure 3. An engineering drawing of the pulsed 8X source. A scale and the magnetic field direction are also shown.

Figure 4. a) An oscillogram of a 25-keV, 37-mA H^- beam from the 8X source. Also shown is the ramp voltage for the emittance scans of this beam displayed in Fig. 4b. The source parameters for this beam are given in column 5 of Table II.

b) X-plane phase space plot for the 25-keV, 37-mA H^- beam shown in Fig. 4a.

Figure 5. a) An oscillogram of a 30-keV, 120-mA H^- beam from the 8X source. Also shown is the ramp voltage for the emittance scans of this beam displayed in Fig. 5b. The source parameters for this beam are given in column 3 of Table II.

b) X-plane phase space plot for the 30-keV, 120-mA H^- beam shown in Fig. 5a.

Figure 6. X-plane phase space plots for a) the 25-keV, 33-mA H^- beam and b) the 30-keV, 30-mA D^- beam. The 8X source parameters for these two beams are given in columns 1 and 2 of Table III.

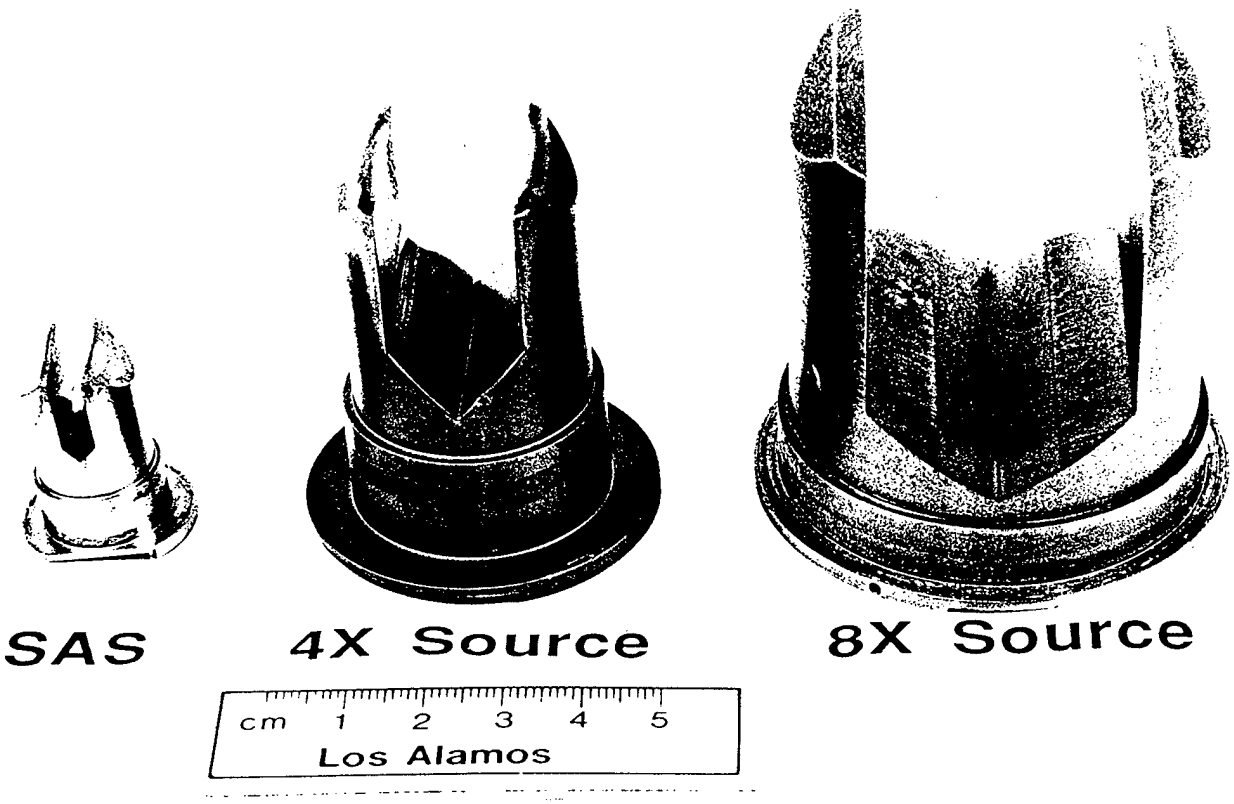

Figure 1

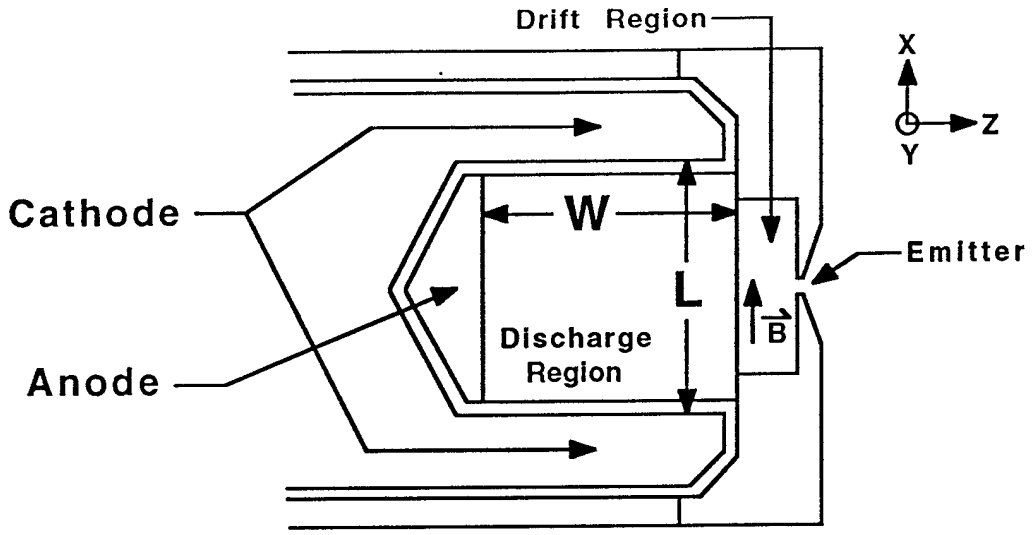
Drift Region
X
Z
Y
Cathode
W
Emitter
L
B
Discharge
Region
Anode

Figure 2

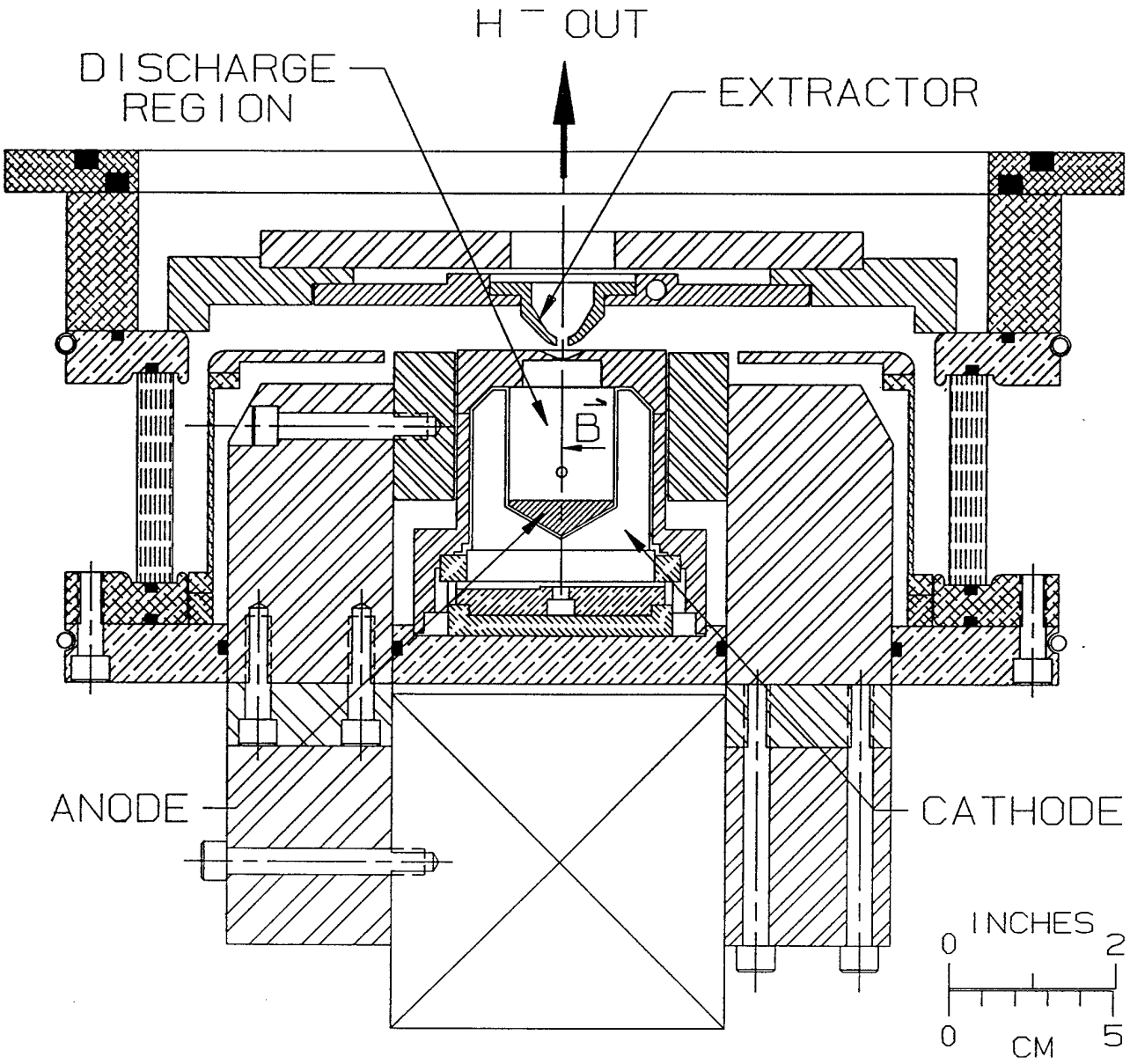
H⁻ OUT
DISCHARGE REGION
EXTRACTOR
B
ANODE
CATHODE
INCHES
0
2
0
CM
5

Figure 3

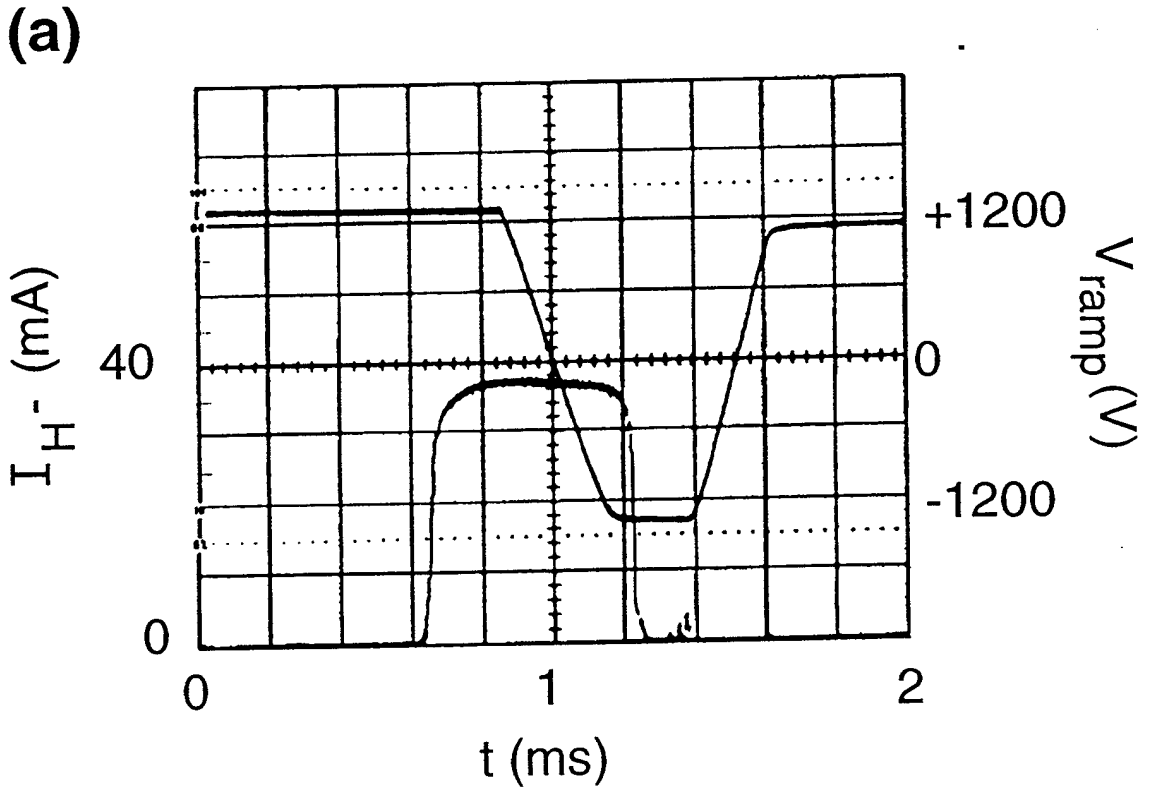

Figure 4 (a)

(b)

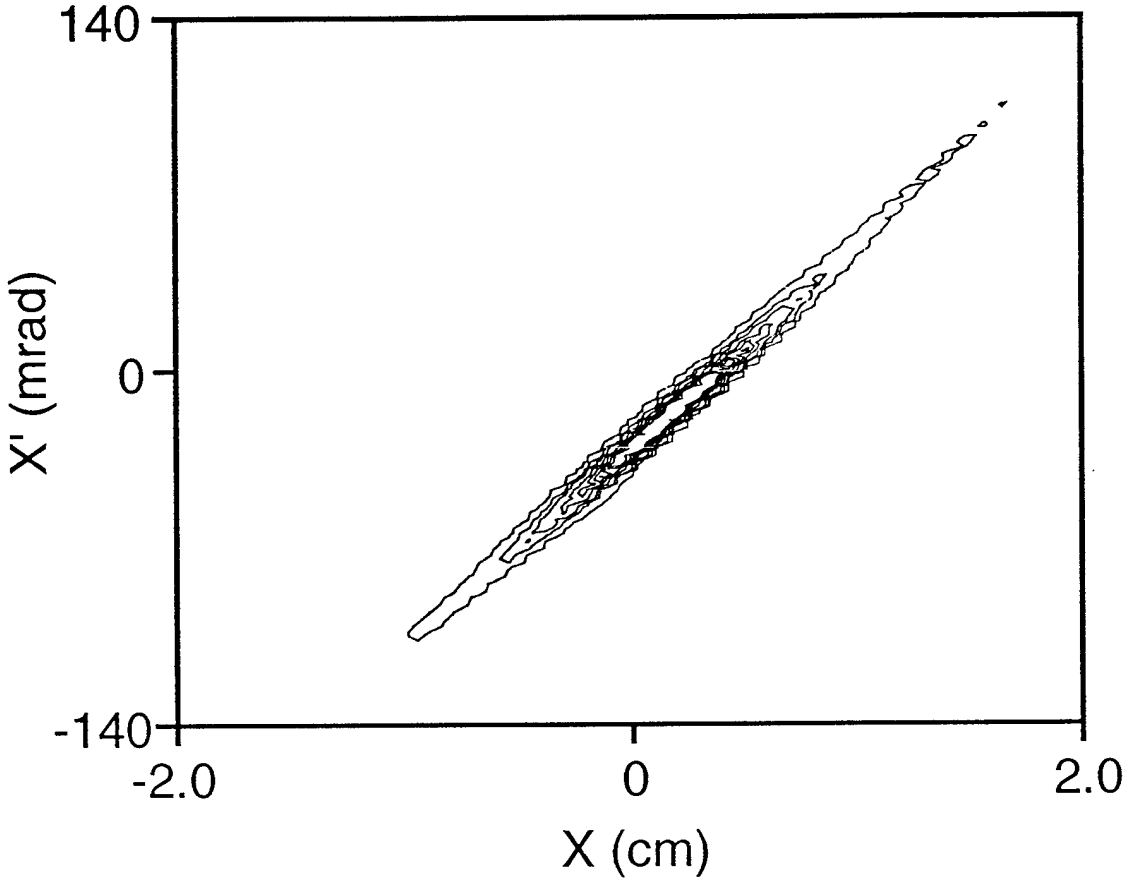

Figure 4 (b)

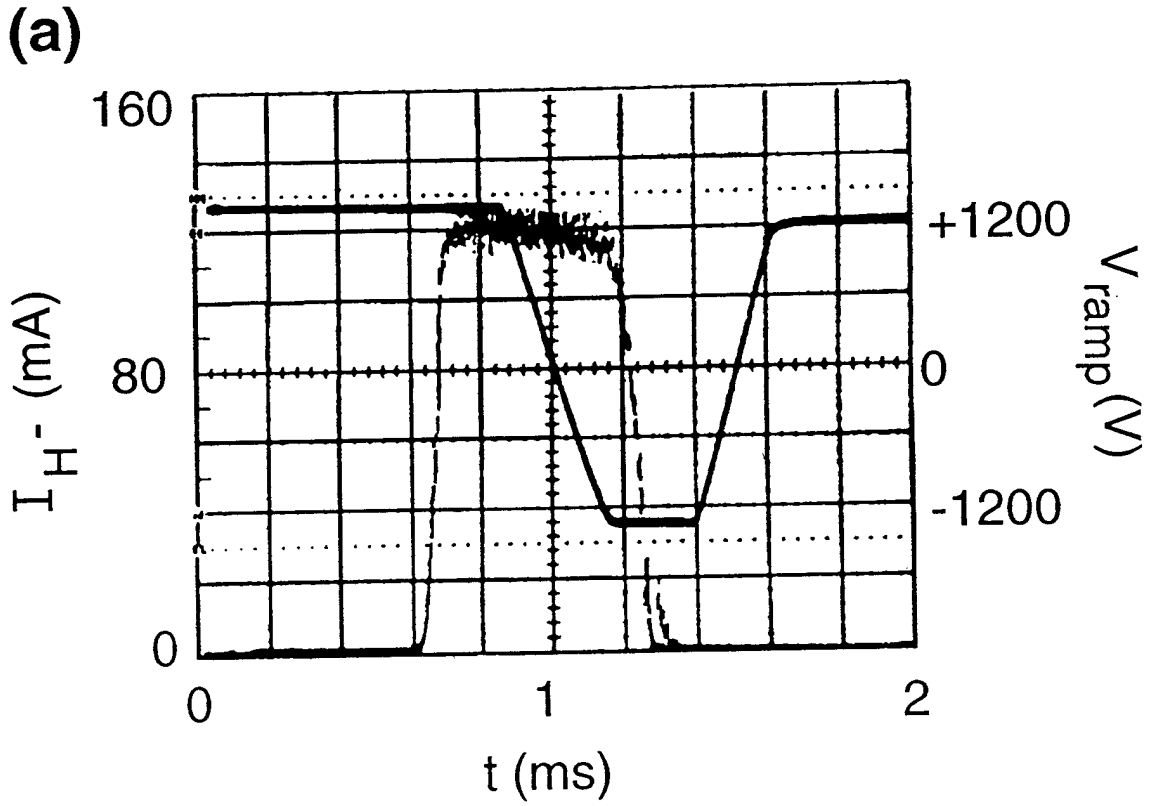

Figure 5 (a)

(b)

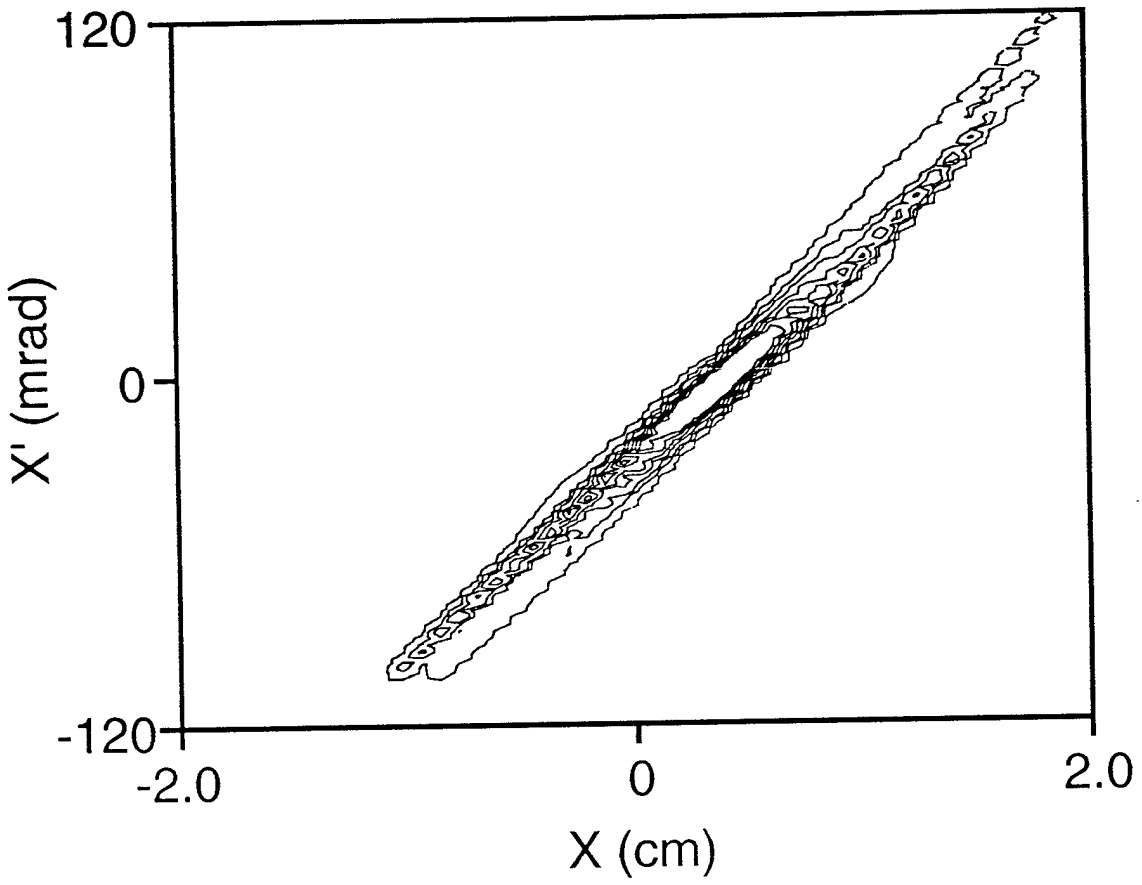

Figure 5 (b)

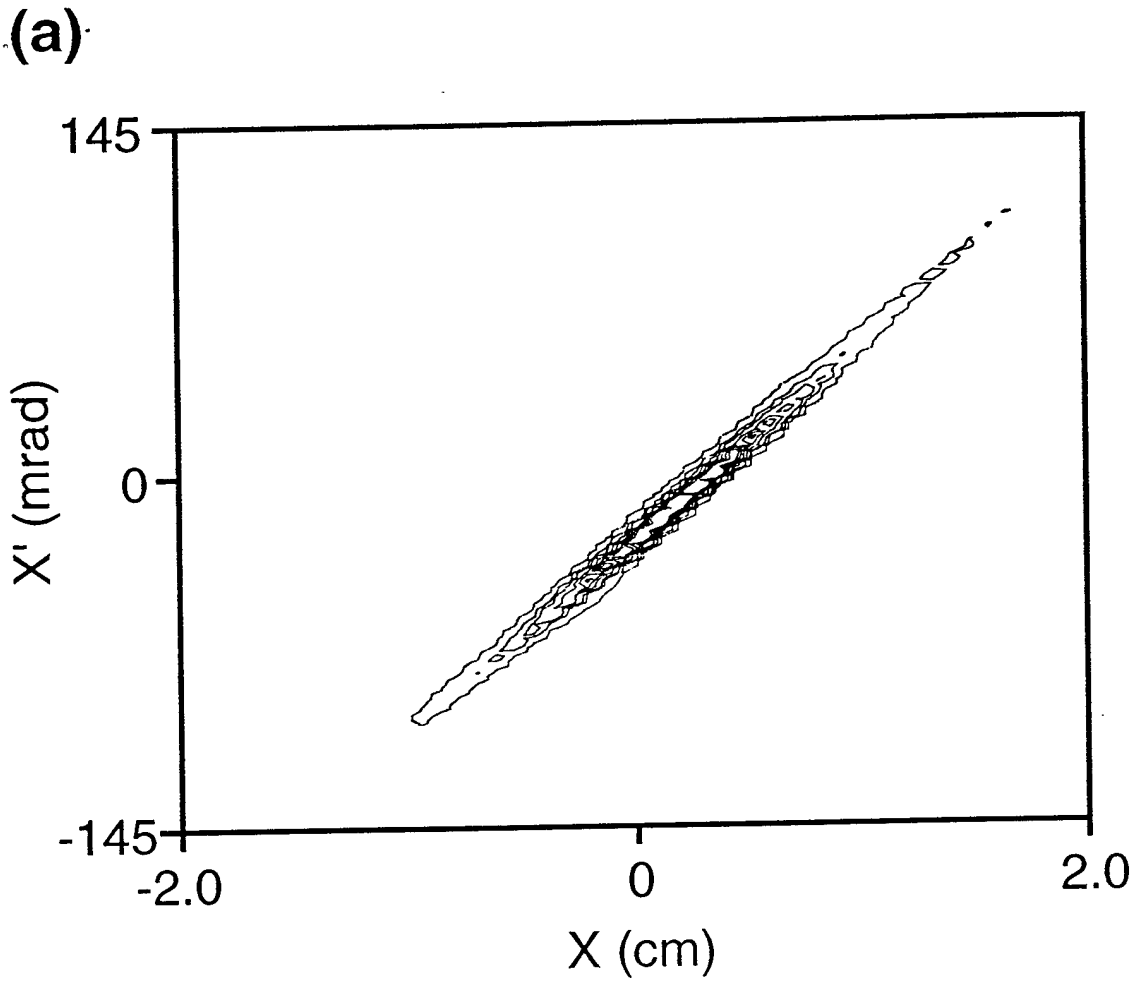

Figure 6 (a)

(b)

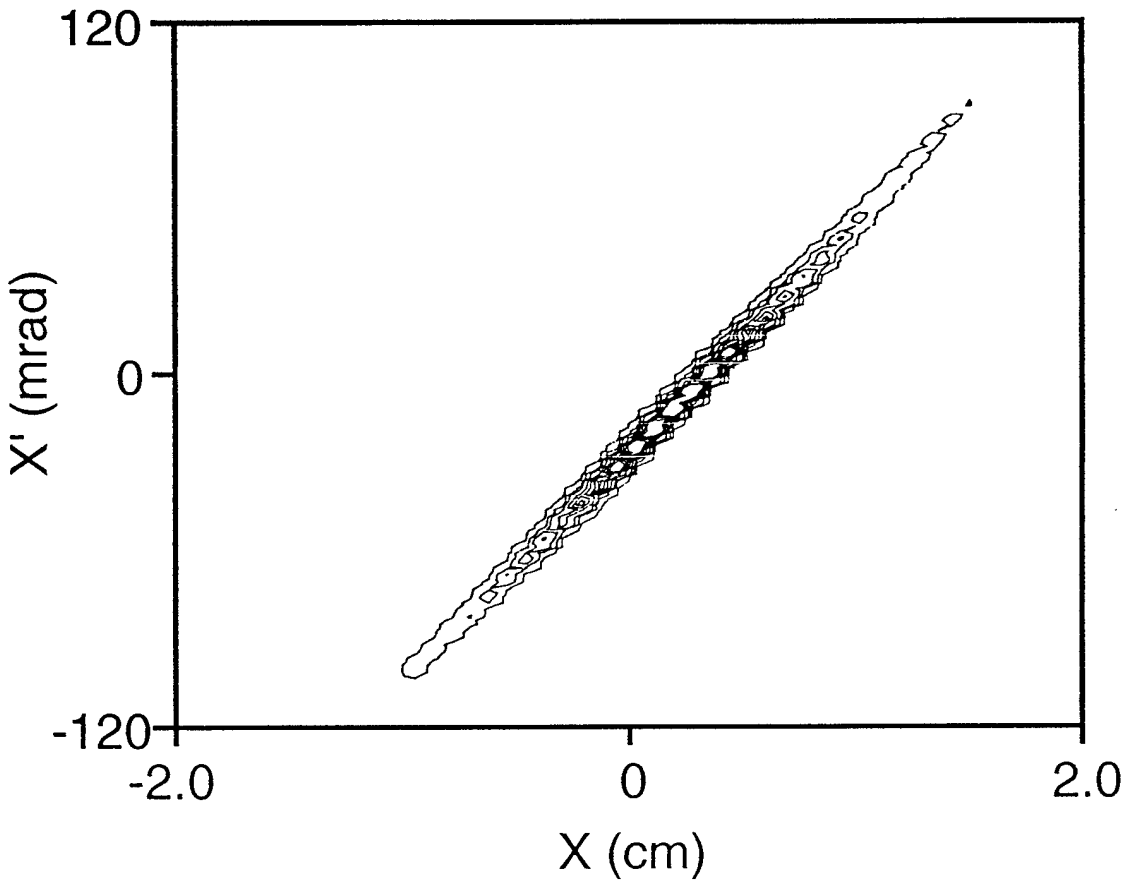

Figure 6 (b)